



Analysis, modeling and design of utility line current conditioner
by Kamalesh Chatterjee

A thesis submitted in partial fulfillment of the requirement for the degree of Master of Science in
Electrical Engineering
Montana State University
© Copyright by Kamalesh Chatterjee (2000)

Abstract:

Data processing devices such as a computer typically feature a diode bridge rectifier at the front end of the power circuit. The diode bridge rectifier, in conjunction with its capacitive filter is a nonlinear load. The device draws current with a high crest factor and rich in harmonics. These harmonic currents cause power quality problems. Such problems have prompted the development of unity power factor rectifiers, which use active current shaping techniques to draw sinusoidal current from the supply. However, such unity power factor rectifiers have not become popular in commercial data processing devices. Incorporating unity power factor rectifier in every device would lead to additional cost. Power quality problems become noticeable only in places where the loading by the data processing devices is substantial part of the total load. There is not enough incentive for the manufacturers to incorporate unity power factor rectifier with every device. Moreover, consumers usually place higher premium in processor speed, memory size, etc.

This thesis presents an alternative approach to solve power quality problems in such scenarios, only when the problems become severe and cause persistent malfunction. The proposed Utility Line Current Conditioner is based on a boost type ac to ac converter topology. The converter would act as an interface between the supply line and the non-linear load. The boost ac-ac converter is adapted to perform line current control in a single-phase line, loaded by a rectifier load. An inner average current control loop and an outer voltage control loop are used to perform the active wave shaping function.

This thesis presents detailed analysis of the basic converter topology, principle of operation, defining equations and design techniques. The dynamic models incorporate high frequency small signal model for the current control loop and a low frequency model for the voltage control loop. The modeling technique is versatile and could be directly applied to ac to dc unity power factor rectifiers as well. Dynamic performance characteristics of the overall system are discussed. Experimental results for a prototype 750 W converter are presented.

ANALYSIS, MODELING AND DESIGN OF UTILITY LINE CURRENT
CONDITIONER

by

Kamalesh Chatterjee

A thesis submitted in partial fulfillment
of the requirement for the degree

of

Master of Science

in

Electrical Engineering

MONTANA STATE UNIVERSITY – BOZEMAN
Bozeman, Montana

April 2000

N378
C3929

APPROVAL

of a thesis submitted by

Kamalesh Chatterjee

This thesis has been read by each member of the thesis committee and has been found to be satisfactory regarding content, English usage, format, citations, bibliographic style, and consistency, and is ready for submission to the College of Graduate Studies.

Giri Venkataramanan

V. Venkatesh

14 APR 2000
Date

Approved for the Department of Electrical Engineering

John Hanton

John Hanton

4-14-00
Date

Approved for the College of Graduate Studies

Bruce McLeod

Bruce S. McLeod

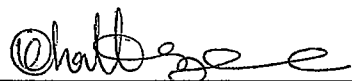
4-24-00
Date

STATEMENT OF PERMISSION TO USE

In presenting this thesis in partial fulfillment of the requirements for a master's degree at Montana State University – Bozeman, I agree that the Library shall make it available to borrowers under rules of the Library.

If I have indicated my intention to copyright this thesis by including a copyright notice page, copying is allowable only for scholarly purposes, consistent with "fair use" as prescribed in the U.S. Copyright Law. Requests for permission for extended quotation from or reproduction of this thesis in whole or in parts may be granted only by the copyright holder.

Signature



Date

April, 17 2000

ACKNOWLEDGMENTS

First and foremost I would like to thank Prof. Giri Venkataramanan for allowing me the opportunity to work on such an exciting project. He gave the initial idea and from the first day he showed immense enthusiasm. He marked the landmarks, warned about possible pitfalls in this project and advised how to avoid them. It was me who often faltered and could not match in enthusiasm. However, the project at its finished form looks wonderful to me. With his assistance in the concepts, in the prototype development and also in the preparation of this thesis he created an excellent and thorough learning opportunity.

I thank NASA, Kennedy Space center, Florida, for their support on this project under the contract number "NAS10-98065". I also thank David Lofftus, MSE Technology Applications, Butte, Montana, for his involvement in this project.

I thank Prof. David Dickensheets for his advice and assistance on various subjects. I owe thanks to other group members Monica Gutierrez and Ji Li for making the Lab time enjoyable. I also thank my other classmates and friends here.

I thank my mother, my brothers and sisters, who in spite of the distance continues to be a source of strength.

TABLE OF CONTENTS

	Page
1. INTRODUCTION	1
2. POWER QUALITY PROBLEMS CAUSED BY RECTIFIER LOADS	5
2.1 Linear Loads and Power Factor.....	5
2.2 Rectifier Loads.....	8
2.3 Experimental Results on Rectifier Loads.....	11
2.4 Possible Solutions to Input Current Harmonics.....	13
2.5 Proposed Ac to Ac Utility Line Current Conditioner.....	17
3. OPERATION OF UTILITY LINE CURRENT CONDITIONER	20
3.1 Power Circuit Topology and Principle of Operation.....	20
3.2 Control Strategy.....	23
3.3 Defining Equations.....	24
3.4 Circuit Averaging and Steady State Solutions.....	27
3.5 Simplified Equivalent Circuit and Steady State Waveforms.....	28
3.6 Equivalent Circuit during Zero Crossing.....	31
3.7 Zero Crossing Spikes in Input Current.....	32
3.8 Proposed Solution to Zero Crossing Spikes.....	34
4. DESIGN ORIENTED ANALYSIS.....	36
4.1 Specifications of the Prototype Converter.....	36
4.2 Boost Inductor Selection.....	37
4.3 Derivation of Power Switch Currents.....	38
4.4 Determination of Blocking Voltages of the Power Switches.....	40
4.5 Semiconductor Switch Selection and other Practical Considerations...41	41

5. HIGH FREQUENCY SMALL SIGNAL MODELING AND ANALYSIS.....	44
5.1 Model of the Basic Boost Converter.....	44
5.2 Average Current Mode Control.....	47
5.3 Modeling the Current Loop.....	48
5.4 Loop Stability and Component Selection.....	50
5.5 Simplified Low Frequency Model of the Current Loop.....	52
6. LOW FREQUENCY DYNAMIC MODELING AND ANALYSIS.....	56
6.1 Control Scheme for Output Voltage Regulation.....	56
6.2 The Overall System including the Rectifier Load.....	57
6.3 Averaged Low Frequency Model.....	58
6.4 Loop Stability of the Voltage Control Loop.....	64
6.5 Closed Loop Output Impedance.....	67
6.6 Small Signal Model and Input Susceptibility.....	68
6.7 Loop Design.....	70
7. EXPERIMENTAL RESULTS.....	72
7.1 Power Circuit and Drive Circuit.....	72
7.2 Control Circuit.....	73
7.3 Prototype Assembly.....	76
7.4 Experimental Results – Waveforms.....	78
7.5 Experimental Results – Performance Analysis.....	81
8. CONCLUSIONS.....	87
REFERENCES.....	91
APPENDICES.....	94
A Power Circuit Design.....	95
B Inductor Design.....	97
C Analysis and Design of the Current Loop.....	99
D Analysis and Design of the Voltage Loop.....	102
E Schematic of the Drive Circuit.....	105
F Schematic of the Control Circuit.....	107
G Steady State Performance Results and Input Current Harmonics.....	109

LIST OF TABLES

	Page
1. Experimental results on rectifier loads.....	11
2. The specifications of the prototype converter.....	36
3. Current controller component values.....	52
4. Voltage controller component values.....	66

LIST OF FIGURES

	Page
2.1 Schematic of an ac supply connected to R-L circuit.....	5
2.2 Voltage and current waveforms of the R-L circuit.....	6
2.3 Voltage and current waveforms of the R-L circuit.....	6
2.4 Schematic of a rectifier load connected to ac supply.....	8
2.5 Output voltage waveform of a bridge rectifier in absence of any other circuit at the output.....	8
2.6 Waveforms of input voltage and input current for a rectifier load.....	9
2.7 Plot of harmonic currents as percentage of fundamental current.....	12
2.8 Schematic of a passive filter used to improve harmonic performance.....	13
2.9 Equivalent circuit of a ferroresonant transformer.....	14
2.10 Block diagram of a ferroresonant transformer with rectifier load.....	14
2.11 Experimental waveforms of a ferroresonant transformer supplying a rectifier load.....	15
2.12 Power circuit of ac to dc unity power factor converter.....	16
3.1 Schematic of the power circuit of utility line current conditioner.....	20
3.2 Control circuit block diagram.....	23
3.3 Equivalent circuit with the S_1 ON S_2 OFF.....	25
3.4 Equivalent circuit with the S_1 OFF S_2 ON.....	26

3.5	Simplified equivalent circuit.....	28
3.6	Simplified steady state waveforms (one complete cycle is 360°).....	30
3.7	(a) Equivalent circuit at zero crossing, (b) Simplified circuit.....	32
3.8	Capacitor voltage and inductor current during resonance.....	33
3.9	Zero crossing spikes in input current (one complete cycle is 360°).....	33
3.10	Normalized steady state waveforms – no zero crossing spike.....	34
4.1	Schematic of the snubber circuit for each mosfet.....	42
4.2	Schematic diagram of complete power circuit.....	43
5.1	Schematic of the boost converter.....	44
5.2	Input and output variables of the boost converter.....	45
5.3	Small signal inputs and outputs of the boost converter.....	46
5.4	A general scheme of average current mode control.....	47
5.5	Current controller using UC3854A.....	48
5.6	The block diagram of the current loop.....	49
5.7	Gain plot of the current loop.....	51
5.8	Phase plot of the current loop.....	51
5.9	Overall gain plot of the current loop.....	53
5.10	Phase plot of the overall transfer function.....	54
5.11	Simplified block diagram of the current loop.....	54
6.1	Block diagram of the control circuit.....	57
6.2	Utility line current conditioner supplying a rectifier type of load.....	58
6.3	Low frequency dynamic model of the utility line current conditioner.....	59

6.4	Equivalent circuit of the load.....	59
6.5	Equivalent circuit of the boost power stage.....	60
6.6	Schematic of the voltage controller.....	62
6.7	Simplified block diagram of voltage control loop for stability analysis.....	64
6.8	Gain plot of the voltage loop.....	65
6.9	Phase plot of the voltage loop.....	66
6.10	Block diagram to determine output admittance.....	67
6.11	Plot of closed loop output impedance.....	68
6.12	Small signal model to determine input susceptibility.....	69
6.13	Plot of small signal input susceptibility.....	69
7.1	The peak detector circuit used in sensing the output voltage.....	74
7.2	Differentiator circuit in the reference current path.....	75
7.3	Reactive current injection scheme.....	76
7.4	The power circuit of the first prototype.....	77
7.5	The second prototype set up.....	77
7.6	Experimental waveforms for input voltage – 110 V, input power - 424 W, output power – 267 W, rectifier type of load with load resistance 140 Ω	78
7.7	Experimental waveforms for input voltage – 110 V, input power - 210 W, output power – 121 W, computer load.....	79
7.8	Experimental waveforms for input voltage – 110 V, input power - 445 W, output power – 359 W, rectifier load with 73 Ω resistance.....	80
7.9	Experimental waveforms for input voltage – 110 V, input power - 391 W, output power – 336 W,	

	resistive load without the rectifier.....	81
7.10	Percentage total harmonic distortion of the input current of the prototype converter as a function of output power.....	82
7.11	Individual harmonics of the input current of the prototype converter.....	83
7.12	Line regulation of the rectified dc voltage of the prototype converter.....	83
7.13	Load regulation of the rectified dc voltage of the prototype converter.....	84
7.14	Efficiency of the prototype converter as a function of output power.....	85

ABSTRACT

Data processing devices such as a computer typically feature a diode bridge rectifier at the front end of the power circuit. The diode bridge rectifier, in conjunction with its capacitive filter is a nonlinear load. The device draws current with a high crest factor and rich in harmonics. These harmonic currents cause power quality problems. Such problems have prompted the development of unity power factor rectifiers, which use active current shaping techniques to draw sinusoidal current from the supply. However, such unity power factor rectifiers have not become popular in commercial data processing devices. Incorporating unity power factor rectifier in every device would lead to additional cost. Power quality problems become noticeable only in places where the loading by the data processing devices is substantial part of the total load. There is not enough incentive for the manufacturers to incorporate unity power factor rectifier with every device. Moreover, consumers usually place higher premium in processor speed, memory size, etc.

This thesis presents an alternative approach to solve power quality problems in such scenarios, only when the problems become severe and cause persistent malfunction. The proposed Utility Line Current Conditioner is based on a boost type ac to ac converter topology. The converter would act as an interface between the supply line and the non-linear load. The boost ac-ac converter is adapted to perform line current control in a single-phase line, loaded by a rectifier load. An inner average current control loop and an outer voltage control loop are used to perform the active wave shaping function.

This thesis presents detailed analysis of the basic converter topology, principle of operation, defining equations and design techniques. The dynamic models incorporate high frequency small signal model for the current control loop and a low frequency model for the voltage control loop. The modeling technique is versatile and could be directly applied to ac to dc unity power factor rectifiers as well. Dynamic performance characteristics of the overall system are discussed. Experimental results for a prototype 750 W converter are presented.

CHAPTER – 1

INTRODUCTION

Electrical power distribution systems almost universally operate as sinusoidal ac voltage sources. The properties of the load determine the amplitude and the waveform of the current drawn from the voltage source. Most lighting loads, heating loads and motor loads are linear loads. When supplied by a sinusoidal voltage source, the current drawn is also sinusoidal. Most data processing devices require dc power source. The dc power is derived from the ac supply by using a rectifier, terminated by a filter. The rectifier-filter is a non linear load. Current drawn from the supply by such loads is not sinusoidal and is rich in harmonics.

Harmonic currents generate electromagnetic interference and affect other devices connected to the same supply line. They also result in degradation of the supply voltage waveform quality. Harmonic currents also result in an increase of rms value of the line current without contributing to the power transfer, resulting in under-utilization of utility installations and increased transmission loss. These degrading effects of harmonic currents become noticeable only when the non-linear loads are a large part of the total load connected to the utility line. With the widespread use of computers and other data processing devices, the contribution of non-linear loads is steadily increasing.

In order to mitigate such problems caused by poor quality of input currents, technology of ac to dc harmonic free rectifiers has become widely available during the last decade. They are often called unity power factor rectifiers or power factor controllers. However, such unity power factor rectifiers have not become popular in commercial data processing devices. Incorporating unity power factor rectifier in every device would lead to additional cost. The power quality problems become noticeable only in places where the loading by the data processing devices is substantial part of the total load. There is not enough incentive for the manufacturers to incorporate unity power factor rectifier with every device. Moreover, consumers usually place higher premium in processor speed, memory size, etc. and not on the supply current waveform quality.

This thesis presents an alternative approach to solve power quality problems in such scenarios. The solution needs to be applied only when the problem becomes severe and causes persistent malfunction of equipment or other equipment connected to the same line. The proposed solution being named as ac to ac Utility Line Current Conditioner (ULCC), is an interface between the utility line and a data processing device such as a computer. The device is used as an add on device only in places where power quality problems demand the additional investment.

ULCC draws sinusoidal current from the supply and regulates the voltage being supplied to the load. It is based on pulse width modulated power converters. They have

been shown to be versatile to perform ac-ac power flow control in various applications [1,2]. The boost ac-ac converter is adapted to perform line current control in a single-phase line, loaded by a rectifier load. An inner average current control loop and an outer voltage control loop are used to perform the active wave shaping function.

Chapter 2 presents a detailed study of the rectifier type of load. Non linear loads such as rectifier loads are studied in detail and measures of harmonic distortion are reviewed. Typical measures of Total Harmonic Distortion (THD) of input current, harmonic currents and current crest factor are provided. Existing solutions to remove harmonic currents are discussed. The concept of the proposed ULCC is introduced.

Chapter 3 presents the power circuit topology of the ULCC. Equivalent circuits and defining equations for different switching intervals are presented. Simplified steady state analytical waveforms are given. During polarity reversal of input line voltage, the zero crossing spike of the input current has been identified as a bottleneck in control and a solution is proposed.

Chapter 4 presents design oriented analysis of the proposed ULCC. From a given set of converter specifications, it presents the equations to select the boost inductor and other circuit elements. Rms and average currents in different branches of the circuit are determined.

Classical circuit averaged model of the boost converter and the control transfer function presented in literature are used to model the average current control loop in Chapter 5. Loop stability and component selection is discussed using Bode plots. A simplified low frequency model of the current loop is introduced.

Chapter 6 presents the dynamic modeling and analysis of the complete system of utility line current conditioner supplying rectifier type of load. The voltage control scheme is discussed in detail. Models of different subsystems are shown separately. Voltage control loop stability is discussed using Bode plots. Closed loop output impedance and input susceptibility are discussed.

A 750 W prototype circuit built to verify the proposed concepts is presented in Chapter 7. Experimental waveforms of input current and other quantities are presented for different type of loads. THD of input current under different load conditions, individual harmonic percentages, line regulation, load regulation and efficiency of the converter are included.

CHAPTER – 2

POWER QUALITY PROBLEMS CAUSED BY RECTIFIER LOADS

Power factor for linear loads is reviewed. Operation of a rectifier type of load is studied in detail. Experimental results of input current waveform are presented. It is shown that input current waveform is rich in harmonics. Crest factor and Total Harmonic Distortion (THD) are defined as a measure of harmonic distortion. Input current harmonics are plotted.

Conventional solutions to improve power quality are discussed. These are: (a) passive filter at the input, (b) ferroresonant transformer, and (c) active power factor correction integrated to the input stage of the rectifier. As a solution to the power quality problems only where it is necessary, the utility line current conditioner is proposed.

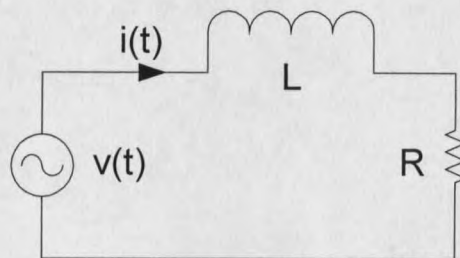
2.1 Linear Loads and Power Factor

Fig. 2.1: Schematic of an ac supply connected to R-L circuit.

Fig. 2.1 presents an ac supply connected to R-L circuit. R is the resistance of the circuit and L is the inductance. At any given instant the value of the supply voltage is $v(t)$ and the current drawn by the load is $i(t)$. The defining equation of the above circuit is

$$L \frac{di(t)}{dt} + Ri(t) = v(t) \quad (2.1)$$

Eq. 2.1 represents a linear differential equation. So, the circuit is called a linear circuit and the R-L load is said to be a linear load. If the supply voltage is a sine wave of some given frequency the input current would also be a sine wave of the same frequency. Since the circuit is inductive the current drawn by the load $i(t)$ would lag the input voltage by an angle (say) θ . Typical voltage and current waveforms are presented in Fig. 2.2. This may also be illustrated in the form of a phasor diagram as shown in Fig. 2.3.

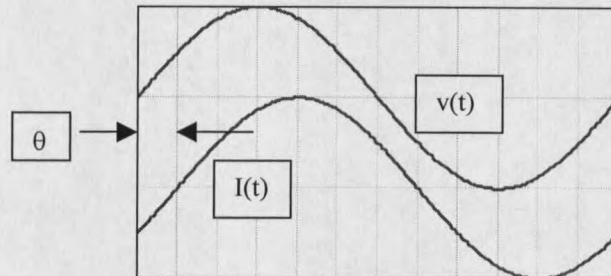


Fig. 2.2: Voltage and current waveforms of the R-L circuit.

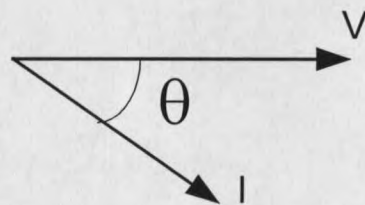


Fig. 2.3: Voltage and current phasor of the R-L circuit.

The average power P drawn by the load per cycle is given by

$$P = \frac{1}{2\pi} \int_0^{2\pi} v(t) i(t) d(\omega t) \quad (2.2)$$

Under such sinusoidal excitation and response conditions as with linear loads, it can be shown that the power P is related to the rms voltage, V_{rms} and the rms current, I_{rms}

$$P = V_{\text{rms}} I_{\text{rms}} \cos(\theta) \quad (2.3)$$

Power factor of the load may be defined as

$$\text{Power factor} = \frac{P}{V_{\text{rms}} I_{\text{rms}}} \quad (2.4)$$

Power factor becomes equal to $\cos(\theta)$ for such linear loads. However, when the load is such that it can not be expressed in terms of linear differential equations, then the load is called non linear. In such cases the current waveform will not be a pure sinusoidal waveform. Since the supply voltage is periodic the current would continue to be periodic and we can define the rms quantities of voltage and current. The definition of power factor as in Eq. 2.4 would be valid. But the power factor would not have a simple interpretation as in the case of linear loads. Rectifier loads are examples of such nonlinear loads and the following section presents a study of rectifier loads.

2.2 Rectifier Loads

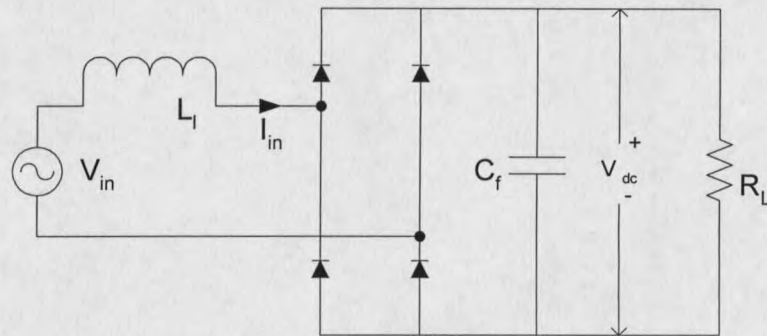


Fig. 2.4: Schematic of a rectifier load connected to ac supply

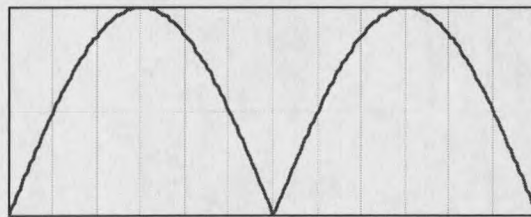


Fig. 2.5: Output voltage waveform of a bridge rectifier in absence of any other circuit at the output.

Fig. 2.4 shows an ac supply connected to a rectifier load. The four diodes connected in the above configuration form a full bridge rectifier. In absence of any other circuit at the output of the rectifier, the output voltage would look like a rectified sine wave as depicted in Fig. 2.5. This waveform, if decomposed into Fourier series, would have a dc component and higher harmonics. A filter is used to remove the harmonics. In Fig. 2.4,

C_f is the filter capacitor. The resistor R_L represents the load. The equivalent inductance of the supply line is shown as L_1 .

The current flows only when the rectifier diodes are forward biased. It is not possible to describe the system operation by linear differential equations as in Eq. 2.1, even if input voltage V_{in} is assumed to be sinusoidal. Fig. 2.6 presents the experimental input current I_{in} of such a rectifier type of load.

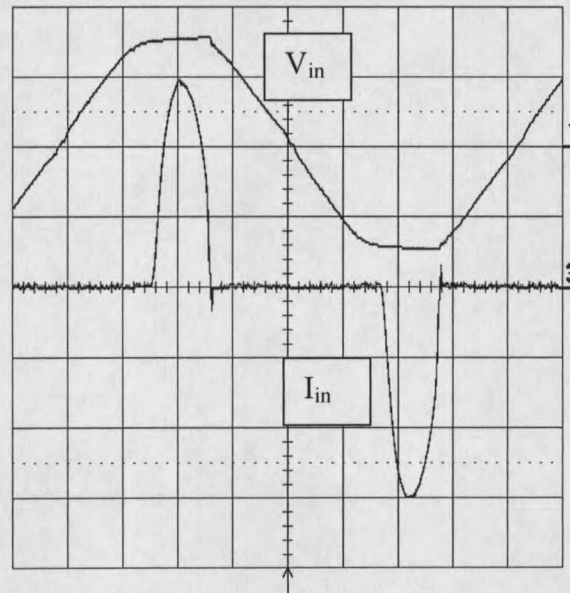


Fig. 2.6: Waveforms of input voltage and input current for a rectifier load.

As seen in Fig. 2.6, there are intervals when the input current is zero. Only when the supply voltage is more than the capacitor voltage, the rectifier diodes are forward biased and the input current builds up. The input current falls when the supply voltage goes below the capacitor voltage. The input current wave shape depends on the inductor L_1

and the loading. If the current waveform were decomposed into different frequency components there would be higher order harmonics along with the fundamental frequency component. It is often said that the current waveform is distorted by the harmonics. Large peak currents increase the rms current more than they contribute to average power. This will result in power factor as defined in Eq. 2.4 to be less than unity. However, following two performance indices better represent the extent of harmonic distortion.

Let the input current peak is denoted by I_p and the rms is denoted by I_{rms} ,

$$\text{Crest factor} = \frac{I_p}{I_{rms}} \quad (2.5)$$

If the current waveform is decomposed into different frequency components and rms value of the fundamental is $I_{rms}(f)$ the Total Harmonic Distortion (THD) as a percentage of fundamental is defined as follows

$$\text{THD} = \frac{\sqrt{I_{rms}^2 - I_{rms}(f)^2}}{I_{rms}(f)} \times 100\% \quad (2.6)$$

For the input current waveform of Fig. 2.6 it is expected that the crest factor and the THD would be large. Both the crest factor and the THD are better measures of harmonic distortion than power factor. As an example, a waveform with a 3% harmonic distortion alone has a power factor of 0.999. A current waveform with 30% total harmonic distortion still has a power factor of 0.95. On the other hand, a current with a 25° phase difference has a power factor of 0.90. Therefore, instead of referring to power

factor, crest factor and THD are often used to evaluate harmonic distortion of a waveform.

2.3 Experimental Results on Rectifier Loads

The circuit shown in Fig. 2.4 was assembled and the experimental results are given in Table 1.

Table - 1 Experimental results on rectifier load

Quantity	Symbol	Value
Circuit parameters/ input quantities		
Load resistor	R_L	140 ohm
Filter capacitor	C_f	2000 μ F
Input voltage	V_{in}	110 V
Test results		
Input power	P_i	158 W
Power factor	pf	0.634
Output dc voltage	V_{dc}	148 V
Input rms current	I_{in}	2.23 A
Input peak current	I_p	5.8 A
Input current crest factor		2.60
Input current THD		117.25%

As anticipated from the waveform, the input current has a large crest factor and a large THD. The individual harmonic currents are plotted in Fig. 2.7.

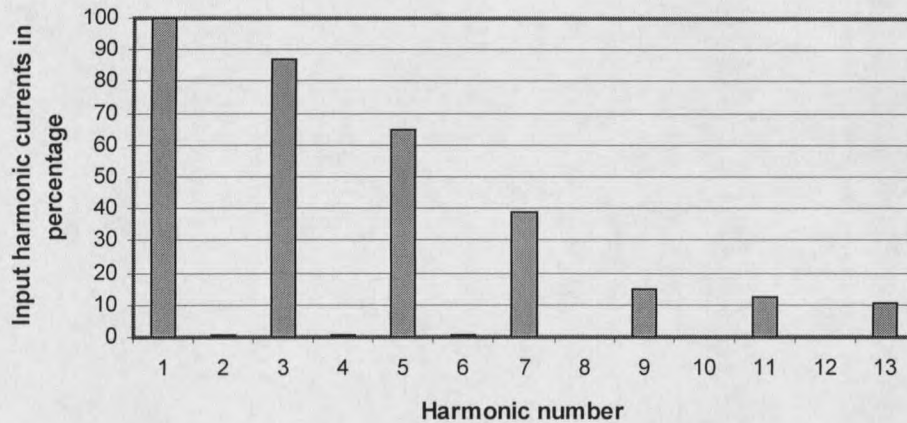


Fig. 2.7: Plot of harmonic currents as percentage of fundamental current.

Input current harmonics not only result in poor power factor but it also affects the other loads connected to the same supply. A typical consequence of high crest factor is that it distorts the voltage waveform and peak voltage gets reduced. High harmonic currents also produce electromagnetic interference. This may affect any sensing or measuring device in the immediate vicinity or connected to the same power line. Over the years, many solutions have been proposed to reduce the input current harmonics. Three such solutions are discussed next.

2.4 Possible Solutions to Input Current Harmonics

2.4 a) Passive Filter at the Input

A passive filter as shown in Fig. 2.8 is connected between the supply line and the rectifier load [3]. It is completely passive and its harmonic performance is good. But it is expensive and bulky. It removes the higher order harmonics but it may have very poor power factor, depending on the loading. This is due to the large series inductor as part of the filter.

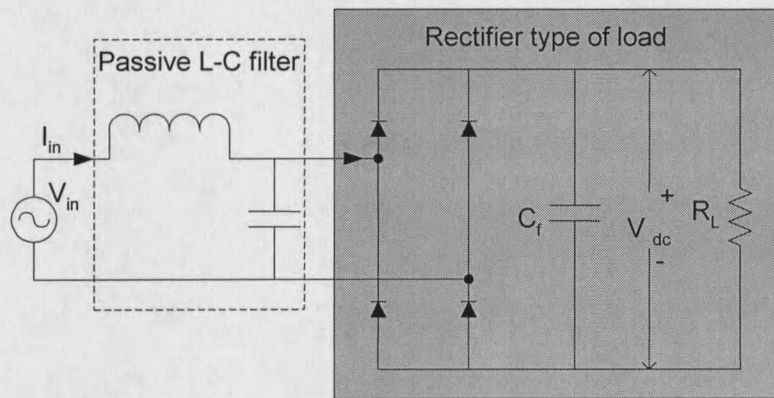


Fig. 2.8: Schematic of a passive filter used to improve harmonic performance.

2.4 b) Ferroresonant Transformer

Ferroresonant transformers are effective in removing higher order harmonics. Most ferroresonant transformers depend on the magnetic saturation and resonant circuits to

achieve this. They also regulate the amplitude of the output voltage. The rms value of the output voltage may change depending on input voltage. Ferroresonant transformers are most useful with rectifier loads in which the dc voltage depends on the amplitude voltage applied to it. Equivalent circuit of a ferroresonant transformer illustrated in Fig. 2.9 shows its basic principle of operation [4]. It differs from a conventional transformer by having a large leakage inductance L_s , a saturating shunt inductance L_p , and a large capacitor in parallel with the load. Fig. 2.10 presents the utilization of a ferroresonant transformer to correct power quality problems.

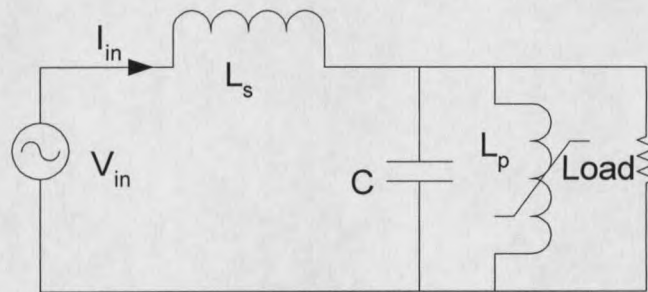


Fig. 2.9: Equivalent circuit of a ferroresonant transformer.

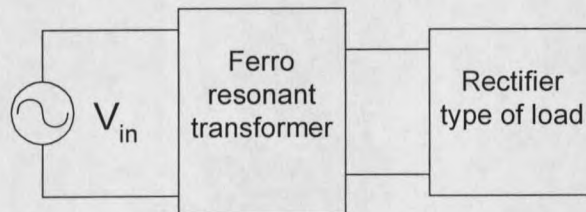


Fig. 2.10: Block diagram of a ferroresonant transformer with rectifier load.

Fig. 2.11 shows the experimental waveforms of a ferroresonant transformer supplying a rectifier load (one personal computer was used). The rectifier input current which is rich in harmonics has been shaped into spectrally cleaner supply line current by the ferroresonant voltage regulator. Because of the presence of large parallel capacitor C in Fig. 2.9 the supply current leads the supply voltage. This is not obvious from Fig. 2.11 because the voltage and current waveforms are taken separately and are at a different time scale. The rectifier input voltage waveform is distorted and it is close to a square wave. However, this does not degrade the performance of the rectifier load, because it is rectified and averaged into dc. Utility line current conditioner proposed later would have similar waveforms of the output voltage.

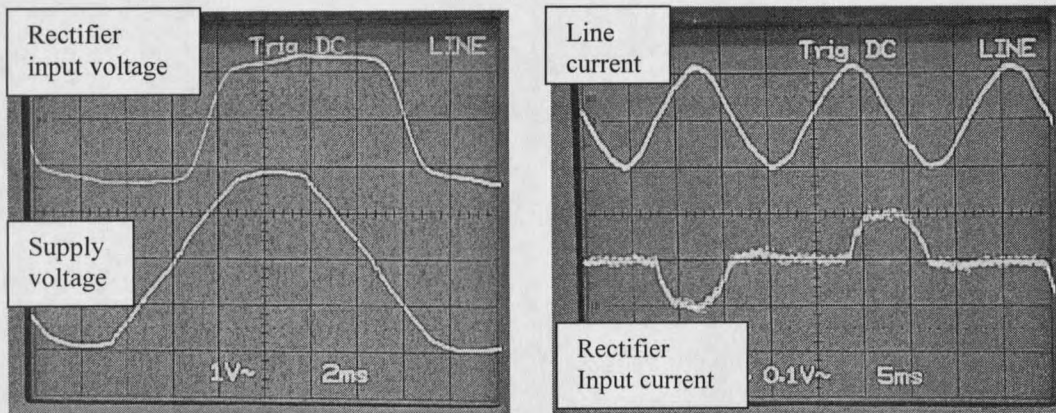


Fig. 2.11: *Experimental waveforms of a ferroresonant transformer supplying a rectifier load.*

2.4 c) Active Power Factor Correction Integrated to the Input Stage of the Rectifier

Over the last ten years this has become the most common scheme for harmonic free (unity power factor) rectification. Reference [5], [6] & [7] present some of the early works in its development. Fig. 2.12 presents the power circuit. It uses a boost converter topology. Supply line is rectified using a full bridge rectifier. High frequency switches S_1 and S_2 are used to control the boost inductor current I_L . S_1 and S_2 are operated as complementary switches. If S_1 and S_2 are used to denote the logic states of the respective switches then the following relation holds.

$$S_1 = \overline{S_2} \quad (2.7)$$

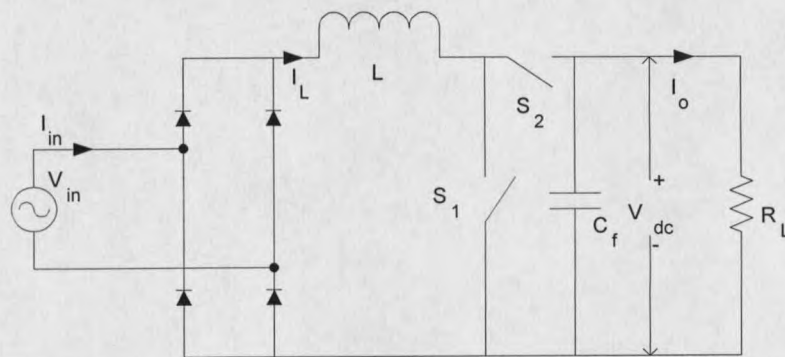


Fig. 2.12: Power circuit of ac to dc unity power factor converter.

Irrespective of the magnitude of supply voltage, when the switch S_1 is closed, the boost inductor L is applied across a positive voltage and current through it increases. After the controlled power switch S_1 is opened, as the complementary switch S_2 is closed, the boost inductor current finds its path through S_2 and charges the filter capacitor C . By controlling the ON-OFF intervals of the controlled switch it is possible to control the

waveform of the current drawn from the supply. This is the basic principle of the circuit operation. The average current mode control scheme is commonly used to control the input current [8]. In averaged current mode control, the inductor current is sensed and compared to the reference current signal to generate a duty ratio command. The current loop variables are continuous and high frequency component is filtered out. However, the filter corner frequency is selected so that it only removes high frequency components and does not interfere with the low frequency components. This in effect, enables the current loop design to use simple state space averaging tools yet gives control over the input current. The disadvantages are the increase in cost for every device and electromagnetic interference generated due to high frequency switching.

2.5 Proposed Ac to Ac Utility Line Current Conditioner

Although the technology of harmonic free unity power factor rectifier is known in the industry for over a decade such rectifiers have not been integrated in commercial data processing devices. Incorporating unity power factor rectifier in every device would lead to additional cost. The power quality problems become severe only in places where the nonlinear loads are a substantial part of the total loading. Moreover, the consumers usually place higher premium in processor speed, memory size, etc. And often the origin of power quality problem goes undetected and if the problem becomes severe isolating transformers or additional filters are installed. In this solution, transformers with delta connected primary windings and star connected four wire

secondary windings are used as isolating transformers. The third harmonic current gets internally circulated and does not enter the primary side. However, this results in overheating of the transformer and it needs to be a high K-factor transformer [9]. This solution is not only very expensive, but it does not address the problem. However, there is no incentive for the manufacturers to incorporate the ac to dc unity power factor rectifier in all data processing devices and not likely to happen in near future.

An alternative solution is proposed herein - ac to ac Utility Line Current Conditioner (ULCC). This device would act as an interface between the supply line and any rectifier load such as a computer. The device may be applied as add on equipment only in places where power quality problems demand the additional investment. The ULCC draws sinusoidal current from the supply and regulates the voltage being supplied to the load. It is based on pulse width modulated converters. They have been shown to be versatile to perform ac-ac power flow control in various applications. The boost ac-ac converter is adapted to perform line current control in a single-phase line, loaded by a rectifier load. The ac line conditioner utilizes an inner average current control loop with an outer voltage control loop to perform the active wave-shaping function. Although this solution would involve additional cost, unlike the unity power factor rectifier, the additional cost need not be added to every data processing device. This solution needs to be applied only when the power quality problem becomes severe and causes persistent malfunction of equipment.

In industry, power converters that provide harmonic free rectification are often called unity power factor converters. Similarly, utility line current conditioner may be called as ac to ac unity power factor converter. These names are commonly used in spite of the fact that power factor is not a good measure of harmonic distortion.

Conclusion

Behavior of linear and non linear loads with respect to input current quality has been studied. Rectifier loads used in most data processing devices have been identified as non linear loads. For such rectifier loads the input current has high crest factor and is rich in harmonics. Several existing solutions to reduce input current harmonics have been discussed. The proposed solution of utility line current conditioner as an add on equipment can be used only in places where power quality problems demand the additional investment. The operation, design and control of the proposed ULCC are presented further in subsequent chapters.

CHAPTER - 3

OPERATION OF UTILITY LINE CURRENT CONDITIONER

Power circuit of the proposed utility line current conditioner is introduced. Operation of the power circuit is explained. Basic design equations are presented. Control strategy based on average current control is proposed. Simplified design equations are solved analytically to produce the steady state waveforms. The chapter concludes with a discussion of zero crossing spike and possible solutions.

3.1 Power Circuit Topology and Principle of Operation

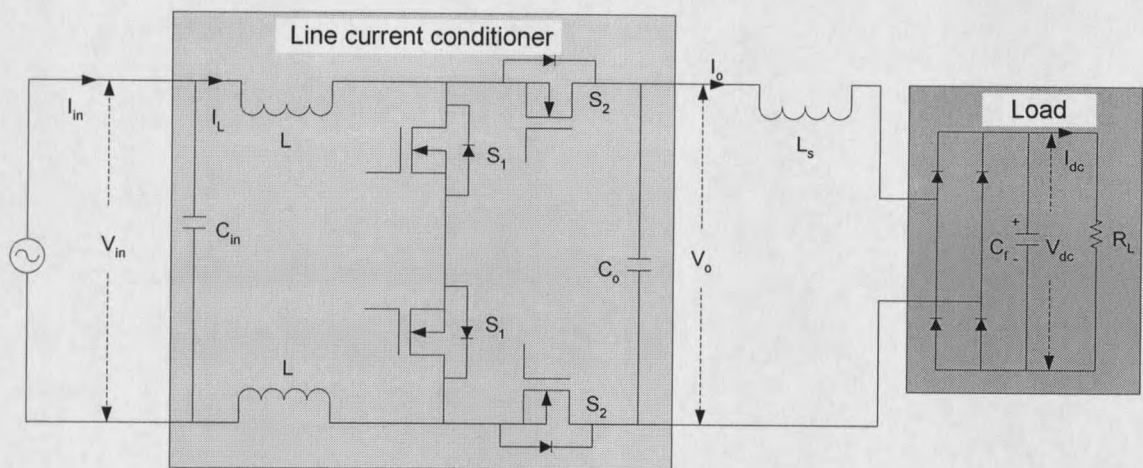


Fig. 3.1: Schematic of the power circuit of utility line current conditioner.

The power circuit of line current conditioner is presented in Fig. 3.1. It shows the line current conditioner, feeding a rectifier type of load. The lightly shaded area on the left is the line current conditioner. Darker shaded area in the right is the data-processing

device, load in this case. The stray inductance L_s accounts for any series inductance present between the output of the utility line current conditioner and the load. The inductors L represent the boost inductor, split into two sections for symmetry. C_f represents the filter capacitor internal to the rectifier. R_L is the equivalent resistance accounting for the loading of the rectifier. C_o and L_s form a second order filter to remove the high frequency component of the switching current. The values of C_o and L_s are selected so that the filter does not attenuate the supply frequency component of the current. The switching ripple in the output current does not affect the performance the utility current conditioner. So, a large switching ripple could be allowed in the output current. Input capacitor C_{in} supplies the high frequency component of the inductor current I_L . Supply frequency component the inductor current is the input current I_{in} . The input current may be controlled to be supply frequency sinusoidal current.

The switches S_1 and S_2 are operated as complementary switches. Their logic states are related by

$$S_2 = \overline{S_1} \quad (3.1)$$

When switches S_1 are closed, the boost inductors appear across the input ac line voltage V_{in} and the inductor current I_L increases in the direction of the input voltage. This current is forced to flow through the load when S_1 switches are opened, and S_2 switches are closed. During this period, the inductor transfers energy to the output capacitor C_o and the inductor current I_L decreases. By suitably controlling the duty ratio of the switches, the inductor current may be maintained at any desired value, as long as the

volt-second balance across the inductor is maintained. The constraint of controlling input current by controlling duty ratio is that the output voltage V_o should be greater in magnitude than the instantaneous value of the input voltage. This constraint is common to boost converter topology. The more stringent constraint is that the output voltage V_o should be of the same sign as the instantaneous value of the input voltage. The consequences of this constraint are discussed in Section 3.7. The relative magnitudes of the input voltage and the output voltage determine the instantaneous duty ratio.

$$V_o(t) = \frac{V_{in}(t)}{1 - D(t)} \quad (3.2)$$

$D(t)$ represents the switching signal, which takes the value of 1 when the switches S_1 are closed and 0 when the switches S_2 are closed. $V_o(t)$ is typically constant over one cycle of the supply frequency, but $V_{in}(t)$ is a sine wave at the supply frequency. So the high frequency averaged value of $D(t)$ is modulated at the supply frequency to maintain the relationship of Eq. 3.2. For simplicity of writing, the notation for time dependence is dropped, but it is to be remembered that all these quantities are modulated at the supply frequency.

The boost converter is operated to control the input current I_{in} to be sinusoidal, proportional to the input voltage so that load to the utility line will appear to be resistive, and hence feature high power factor. Average current control technique is used to achieve this. Average current mode control is most commonly used for a wide variety of converter topologies. In average current mode control, the current controller

does not directly generate the switching signal, instead it produces the average value of the switching signal which is used to generate a pulse width modulated gate drive waveform.

3.2 Control Strategy

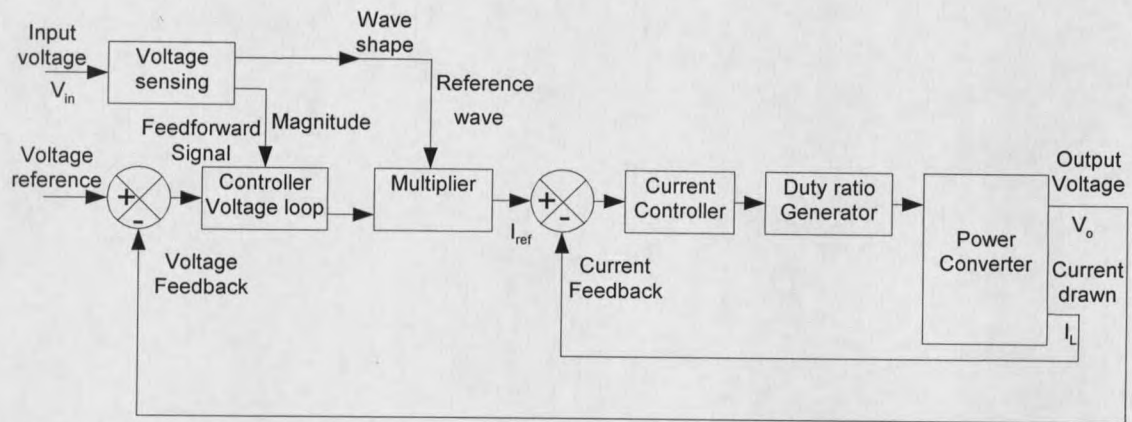


Fig. 3.2: Control circuit block diagram.

A block diagram of the control circuit is presented in Fig. 3.2. The inductor current I_L is sensed and compared to the reference current I_{ref} . The inner current control loop modifies the duty ratio of the boost converter to maintain the current through the boost inductor at the reference value.

The reference current is modulated to follow the input voltage waveform. If the current loop is fast enough, the current drawn by the converter will follow the reference current, and hence the input voltage, thereby providing unity power factor operation. The bandwidth of the current loop should be much larger than the supply frequency 60 Hz,

typically more than 1 kHz. If the current loop gain includes a pole at the zero frequency, this will act as an integrator and eliminate dc errors.

The output voltage feedback controller provides the magnitude command for the inner current control loop. A multiplier is used to generate the instantaneous value of the reference current command from the voltage error amplifier and the input voltage waveform. The voltage loop changes the magnitude of the reference current command depending on the loading and maintains the required output voltage. Voltage loop needs to be slow enough not to modulate the reference current waveform with second and third harmonic being fed back from the measured rectified waveform.

3.3 Defining Equations

S_1 and S_2 are controlled power switches, they can pass bi-directional current and block unidirectional voltage. S_1 and S_2 are complementary switches as in Eq. 3.1. S_1 ON or S_2 ON will result in two different equivalent circuits. The system alternates between these two equivalent circuits at switching frequency (50 kHz).

3.3 a) With S_1 ON S_2 OFF, Rectifier Conducting

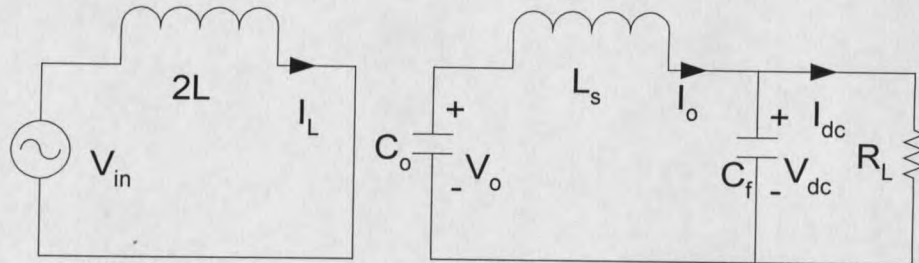


Fig. 3.3: Equivalent circuit with the S_1 ON S_2 OFF.

Equivalent circuit with S_1 ON and rectifier conducting is presented in Fig. 3.3. The switch and the diode drop and other non-idealities are neglected. In this interval the boost inductors are shorted and current through them increases in the direction of V_{in} . Output stage is disconnected from the input stage in this interval.

The defining equations for this interval are given below.

$$\frac{dI_L}{dt} = \frac{V_{in}}{2L} \quad (3.3a)$$

$$\frac{dV_o}{dt} = \frac{-I_o}{C_o} \quad (3.3b)$$

$$\frac{dI_o}{dt} = \frac{V_o - V_{dc}}{L_s} \quad (3.3c)$$

$$\frac{dV_{dc}}{dt} = \frac{I_o - I_{dc}}{C_f} \quad (3.3d)$$

3.3 b) With S_1 OFF S_2 ON, Rectifier Conducting

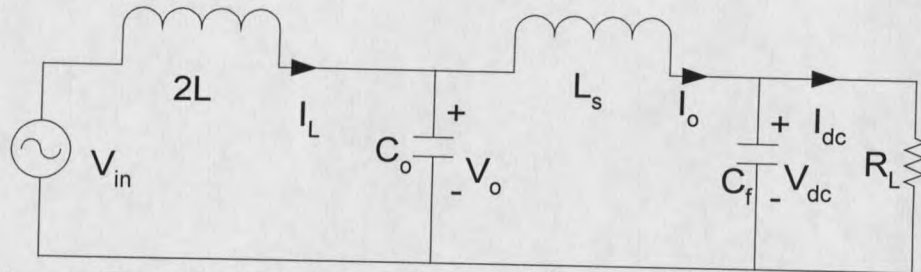


Fig. 3.4: *Equivalent circuit with the S_1 OFF S_2 ON.*

The equivalent circuit with S_2 ON and rectifier conducting is presented in Fig. 3.4. In this interval the boost inductors are charging the capacitor C_o .

The defining equations for this interval are given below.

$$\frac{dI_L}{dt} = \frac{V_{in} - V_o}{2L} \quad (3.4a)$$

$$\frac{dV_o}{dt} = \frac{I_L - I_o}{C_o} \quad (3.4b)$$

$$\frac{dI_o}{dt} = \frac{V_o - V_{dc}}{L_s} \quad (3.4c)$$

$$\frac{dV_{dc}}{dt} = \frac{I_o - I_{dc}}{C_f} \quad (3.4d)$$

3.4 Circuit Averaging and Steady State Solutions

The above equations describe the overall system. Assuming the switching frequency is much larger than the circuit time constants, the switching variable is replaced with a continuous variable D [10]. This is the duty ratio D as in Eq. 3.2. Time average of the switching variable is the duty ratio D . This is also called circuit averaging technique. Reference [11] provides a comprehensive treatment of the subject.

$$\frac{dI_L}{dt} = \frac{V_{in} - (1-D)V_o}{2L} \quad (3.5a)$$

$$\frac{dV_o}{dt} = \frac{I_L(1-D) - I_o}{C_o} \quad (3.5b)$$

$$\frac{dI_o}{dt} = \frac{V_o - V_{dc}}{L_s} \quad (3.5c)$$

$$\frac{dV_{dc}}{dt} = \frac{I_o - I_{dc}}{C_f} \quad (3.5d)$$

Neglecting the effects of the small intervals when the bridge rectifier is not conducting the steady state solutions could be found by equating these state variable derivatives to zero. Considering a small values of filter components L_s and C_o ,

$$V_o = \frac{V_{in}}{1-D} \quad (3.6a)$$

$$I_L = \frac{I_o}{1-D} \quad (3.6b)$$

$$V_o(\text{peak}) = V_{dc} \quad (3.6c)$$

$$I_o(\text{average}) = I_{dc} \quad (3.6d)$$

3.5 Simplified Equivalent Circuit and Steady State Solutions

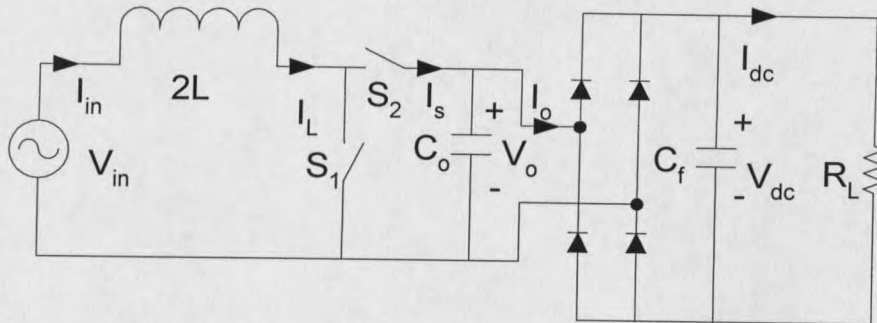


Fig. 3.5: Simplified equivalent circuit.

Fig. 3.5 presents the simplified equivalent circuit. Input filter capacitor and output stray inductor are ignored.

If V_{in} is a sine wave of frequency ω ,

$$V_{in}(t) = V_m \sin(\omega t) \quad (3.7)$$

and the boost ratio k is defined as,

$$k = \frac{V_m}{V_{dc}} \quad (3.8)$$

Then the average duty ratio $D(t)$ could be expressed as,

$$D(t) = \frac{V_o(t) - V_{in}(t)}{V_o(t)} \quad (3.9)$$

$$D(t) = 1 - k|\sin(\omega t)| \quad (3.10)$$

And the average switch current $I_s(t)$ is given by,

$$\text{Average } I_s(t) = I_{in}(t) \times \{1 - D(t)\} \quad (3.11)$$

$$\text{Average } I_s(t) = I_m k \sin(\omega t) |\sin(\omega t)| \quad (3.12)$$

The simplified waveforms are presented in Fig. 3.6. The time axis is indicated as normalized time, this means one complete supply frequency cycle is shown as 360° . If the current control loop of the boost stage works properly, I_{in} could be assumed to be a sine wave in phase with V_{in} as shown in Fig. 3.6. The third waveform is the average duty ratio $D(t)$ as described by Eq. 3.10. Next is average value of the switched current $I_s(t)$, this has the square of a sine wave shape as described in Eq. 3.12. Next is $V_o(t)$ having a peak equal to V_{dc} , when the rectifier is conducting this will be equal to V_{dc} . For simplicity V_{dc} is assumed to be constant here. For the first $1/6$ cycle time, the output voltage V_o changes sign and rectifier is not conducting. This mode starts whenever V_{in} changes polarity. During this time $I_o(t) = 0$. Input current charges the capacitor in the opposite polarity. This mode stops when $|V_o|$ becomes equal to V_{dc} . $I_o(t)$ becomes equal to $I_s(t)$ when the rectifier conducts.

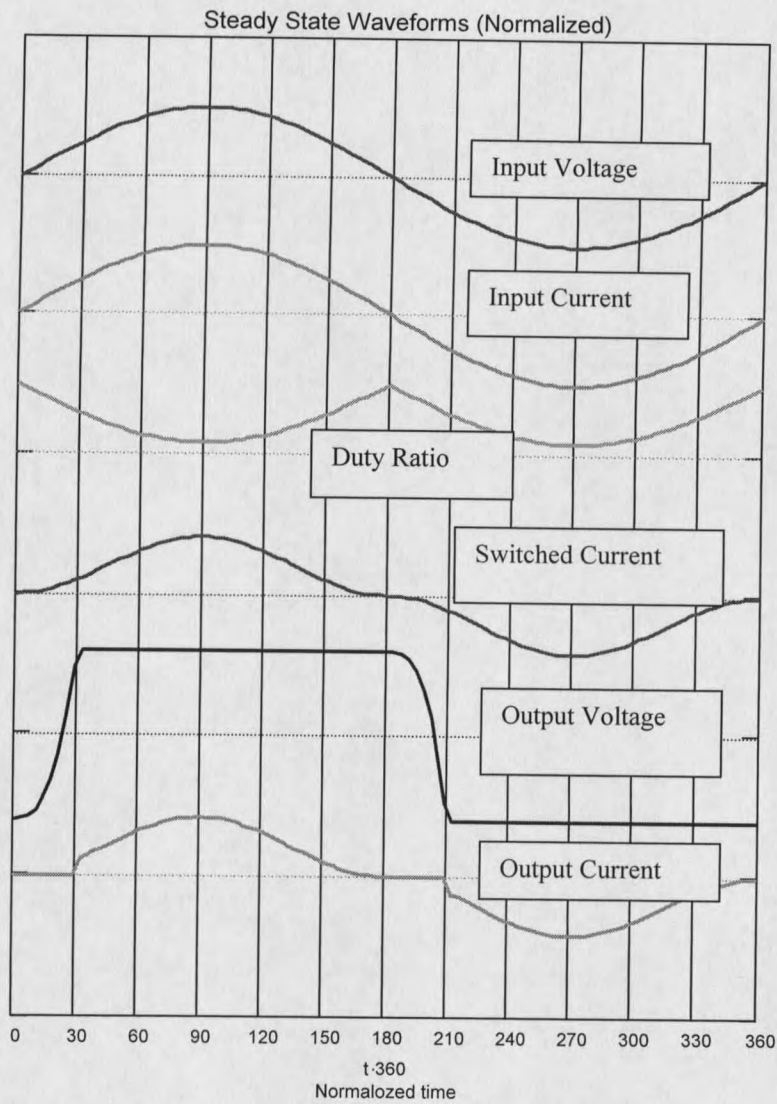


Fig. 3.6: Simplified steady state waveforms (one complete cycle is 360°).

These waveforms demonstrate the operation of the proposed circuit. These waveforms are solutions to the simplified equations developed herein. In Chapter 7 the experimental waveforms are presented that verify these results.

3.6 Equivalent Circuit during Zero Crossing

From the discussion of Section 3.4, when the input voltage V_{in} and output voltage V_o are of opposite polarity then Eq. 3.6a does not have a viable steady state solution. This is because D is limited between zero and one. So, during this interval the circuit loses control over the inductor current. This condition occurs whenever the input voltage changes polarity. When the input voltage changes polarity the output voltage also will change polarity and the bridge rectifier will not conduct until the capacitor C_o gets charged to V_{dc} of the opposite polarity. This is seen in Fig. 3.6 between 180° and 210° . However, since the control circuit has lost control over inductor current there will be resonance between the boost inductors and the output capacitor C_o and this will decide the input current. This will result in large current spike of the inductor current I_L and I_{in} .

The equivalent circuit from the output side during zero crossing resonance is presented in Fig. 3.7a and is simplified as shown in Fig 3.7b. The rectifiers are reverse biased so the load is disconnected. During zero crossing D is very close to unity, this makes the effective inductance very small. This results in a large current spike as will be discussed further.

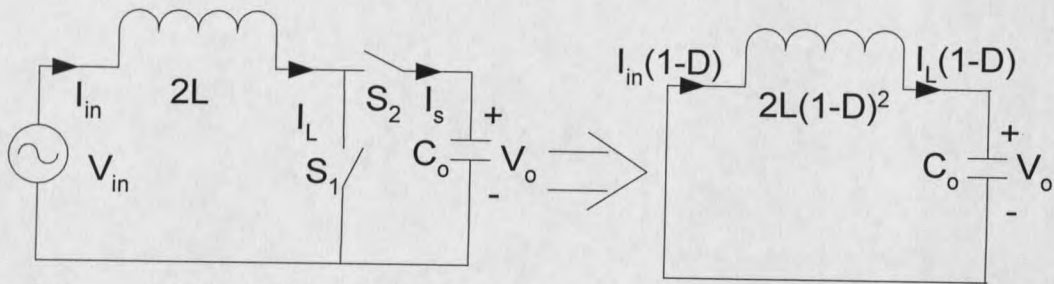


Fig. 3.7: a) Equivalent circuit at zero crossing. b) Simplified circuit.

3.7 Zero Crossing Spikes in Input Current

Fig. 3.7b is an L-C resonant circuit and at the end of the resonance the capacitor will have its charge reversed. In Fig. 3.8 the resonance interval is studied and it is observed that the capacitor voltage changes polarity at the end of the resonance interval when the control circuit resumes its control over the inductor current. The time scale of Fig. 3.8 is small compared to the total cycle time. The large current spike will distort the input current waveform as shown in Fig. 3.9.

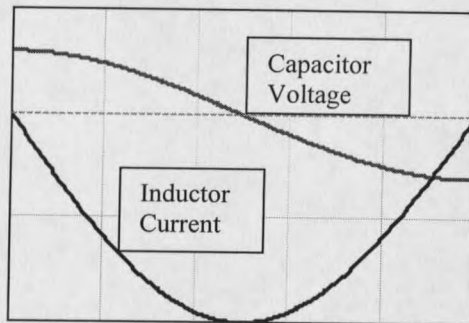


Fig. 3.8: Capacitor voltage and inductor current during resonance.

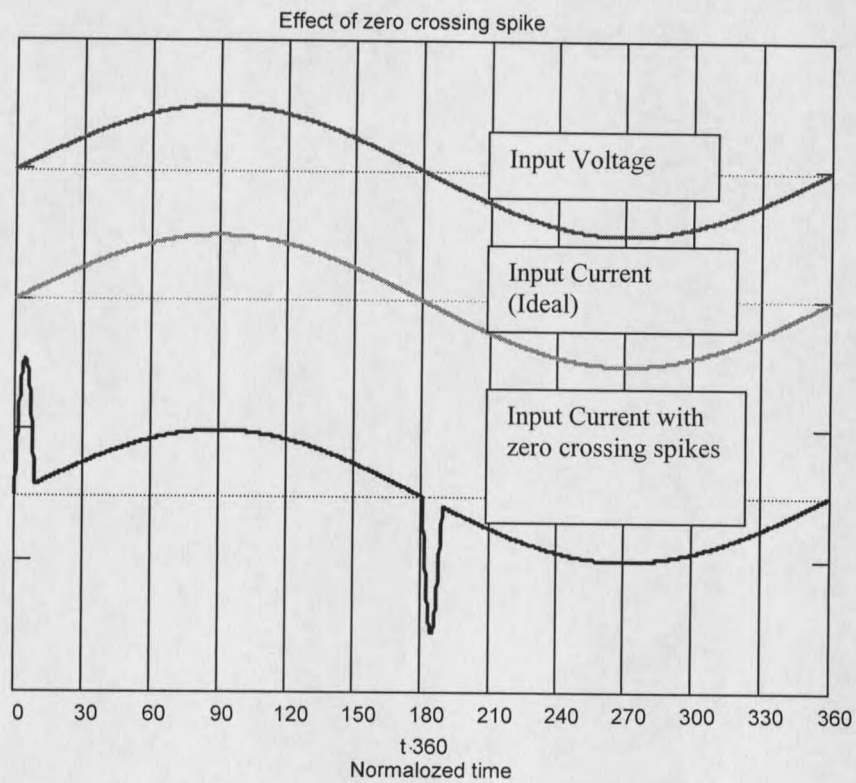


Fig. 3.9: Zero crossing spikes in input current (one complete cycle is 360°).

3.8 Proposed Solution to Zero Crossing Spikes

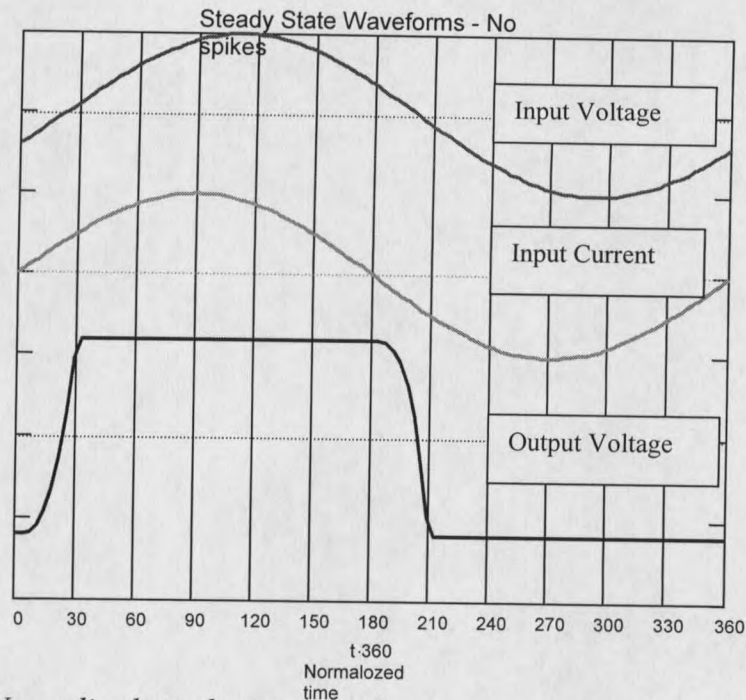


Fig. 3.10: Normalized steady state waveforms – no zero crossing spike.

In the simplified equivalent circuit of Fig. 3.5, direction of current can be controlled to any positive or negative values independent of input voltage polarity as long as duty ratio has control over input current. If a phase lead between the input voltage and the reference current signal is introduced, then the input current will become negative before the input voltage becomes negative. This negative current can change the polarity of the output capacitor. This is illustrated in Fig. 3.10. If the amount of phase lead is such that the input voltage and the capacitor voltage changes polarity at the same time, there will be no spikes in the input current as shown in Fig. 3.10.

The required phase difference will depend on the loading and the circuit parameters. This phase difference needs to be accurate over all loads to make zero crossing spikes disappear. It is possible to design simple analogue circuits, which can be tuned to operate under a given set of operating conditions. It is desirable to have digital controller and a dynamic phase lead adjustment algorithm, which adjusts the phase lead in real time to eliminate the spikes for better performance.

Conclusion

The power circuit operation for the proposed utility line current conditioner has been explained in this chapter. The defining equations have been developed from the equivalent circuits. The defining equations are solved analytically and simplified steady state waveforms have been presented. These will enable the design of the power circuit components of the prototype, which is presented in the next chapter.

CHAPTER – 4

DESIGN ORIENTED ANALYSIS

This chapter presents design oriented analysis of the ULCC. With the help of the steady state equations derived in the last chapter, design equations are presented here. Selection of the boost inductor and the switch average and rms currents are presented. The ideal power switches are realized with the available power MOSFETs. A complete circuit diagram of the power circuit is given.

4.1 Specifications of the Prototype Converter

Table 2 presents the specifications of the prototype converter built to verify the concepts. The rectified dc voltage, V_{dc} , has to be higher than the peak of the maximum input voltage. V_{dc} is chosen to be 200 V to provide a reasonable amount of margin under overvoltage conditions. Selection of the boost inductor and the power semiconductor switches are explained for the following specifications.

Table - 2 The specifications of the prototype converter

Quantity	Symbol	Value
Output power	P_o	750 W
Input voltage	V_{in}	100-130 V
Dc bus voltage	V_{dc}	200 V
Switching frequency		50 kHz
Supply frequency		60 Hz

4.2 Boost Inductor Selection

When supply voltage is at its minimum, the amount of boosting necessary is maximum and the current stress on the inductor is maximum. Thus, the minimum rms supply voltage is the condition used for developing the inductor selection methodology.

$$V_{in} = V_{in}(\min) = 100V \quad (4.1)$$

The input power is determined assuming some efficiency (say) $\eta = 90\%$

$$P_{in} = P_o / \eta \quad (4.2)$$

The rms input current may be determined as

$$I_{in} = P_{in} / V_{in} \quad (4.3)$$

And the peak input current is given by

$$I_{pk} = \sqrt{2} I_{in} \quad (4.4)$$

The duty ratio can be determined from the input and output voltages. The duty ratio D at the peak of the input voltage is

$$D = \frac{V_{dc} - \sqrt{2} V_{in}}{V_{dc}} \quad (4.5)$$

At the peak of the input voltage a certain ripple current, $\Delta I =$ (say) 20% is assumed.

The boost inductor may be calculated from the ripple current specifications as [11].

$$L = \frac{1}{2} \frac{\sqrt{2} V_{in} \times D}{f_s \times \Delta I} \quad (4.6)$$

The boost inductor selection is presented in detail. Selection of other power circuit components is presented in Appendix A as a Microsoft Excel[®] design sheet. Appendix B presents the Mathcad[®] sheet for inductor design. The formulas of determining the worst case rms and average currents in the switches S_1 and S_2 are presented below.

4.3 Derivation of Power Switch Currents

4.3 a) Average and Rms Current through S_1

Half cycle average current of the switch S_1 is given by

$$I_{s1(av)} = \frac{1}{\pi} \int_0^{\pi} I_{s1}(t) dt \quad (4.7)$$

where $I_{s1}(t)$ is the instantaneous current through S_1 . $I_{s1}(t)$ could be expressed as

$$I_{s1}(t) = I_{in}(t) D(t) \quad (4.8)$$

Combining the above two equations and substituting $D(t)$ from Eq. 3.9c,

$$I_{s1(av)} = \frac{1}{\pi} \int_0^{\pi} I_m \sin(\omega t) \{1 - k \sin(\omega t)\} d(\omega t) \quad (4.9)$$

where I_m is the peak of the input current and the boost ratio k is defined by

$$k = \frac{\sqrt{2} V_{in}}{V_o} \quad (4.10)$$

Performing the integral in Eq. 4.9 the average switch current may be obtained to be

$$I_{s1}(\text{av}) = I_m \left\{ \frac{2}{\pi} - \frac{k}{2} \right\} \quad (4.11)$$

This may be expressed in terms of input average current $I_{in}(\text{av})$ as

$$I_s(\text{av}) = I_{in}(\text{av}) \left(1 - k \frac{\pi}{4} \right) \quad (4.12)$$

It is straightforward to modify Eq. 4.9 to get the rms current $I_{s1}(\text{rms})$.

$$I_{s1}(\text{rms})^2 = \frac{1}{\pi} \int_0^{\pi} \{I_m \sin(\omega t)\}^2 \{1 - k \sin(\omega t)\} d(\omega t) \quad (4.13)$$

Evaluation of the integral results in

$$I_{s1}(\text{rms}) = I_m \sqrt{\frac{1}{2} - \frac{4k}{3\pi}} \quad (4.14)$$

This result is expressed in terms of input rms current.

$$I_{s1}(\text{rms}) = I_{in}(\text{rms}) \sqrt{1 - k \frac{8}{3\pi}} \quad (4.15)$$

4.3 b) Average and Rms Current through S_2

The average current through S_2 , $I_{s2}(\text{av})$ could be calculated following the same procedure as above and modifying Eq. 4.8 and Eq. 4.9. However, the average the

current through the capacitors C_o or C_f has to be zero in steady state. This leads to direct answer for $I_{s2(av)}$

$$I_{s2(av)} = I_o \quad (4.16)$$

Eq. 4.8 is modified for switch S2 as

$$I_{s2}(t) = I_{in}(t) \{1 - D(t)\} \quad (4.17)$$

The expression for rms current is given by

$$I_{s2}(rms)^2 = \frac{1}{\pi} \int_0^{\pi} \{I_m \sin(\omega t)\}^2 \{k \sin(\omega t)\} d(\omega t) \quad (4.18)$$

Evaluation of the integral and simplification results in

$$I_s(rms) = I_{in}(rms) \sqrt{k \frac{8}{3\pi}} \quad (4.19)$$

4.4 Determination of Blocking Voltages of the Power Switches

With reference to the ideal power circuit as shown Fig. 3.1, S_1 blocks when the switch S_2 conducts. So the blocking voltage for switch S_1 , $V_1(OFF)$ is the output voltage V_o . Peak value of V_o could be considered as approximately equal to V_{dc} if the rectifier diode drops are neglected.

$$V_1(\text{OFF}) = V_{dc}(\text{peak}) \quad (4.20)$$

Similarly blocking voltage for switch S_2 , $V_2(\text{OFF})$ is approximately equal to V_{dc} .

$$V_2(\text{OFF}) = V_{dc}(\text{peak}) \quad (4.21)$$

Equations 4.20 and 4.21 are valid only in ideal cases. In practice the switches are not ideal, so the dead time considerations and the voltage spike due to stray inductance would necessitate the selection of power switches of much higher voltage rating. The necessity of the dead time when both the switches S_1 and S_2 are OFF is explained in the next section. It is also shown that a turn OFF snubber is necessary to provide an alternate path for the inductor current during the dead time.

4.5 Semiconductor Switch Selection and other Practical Considerations

Each power switch in Fig. 3.1 needs to block unidirectional voltage and pass bi-directional current. The relevant power switches for this application are IGBT and MOSFET. For low power applications MOSFET is recommended and for high power applications use of IGBT is recommended. For the specifications given, the above power MOSFET could be used. To select the MOSFET one needs to know the peak rms current stress and the voltage stress. Equations (4.12-4.19) present the formulas for calculating average and the rms currents.

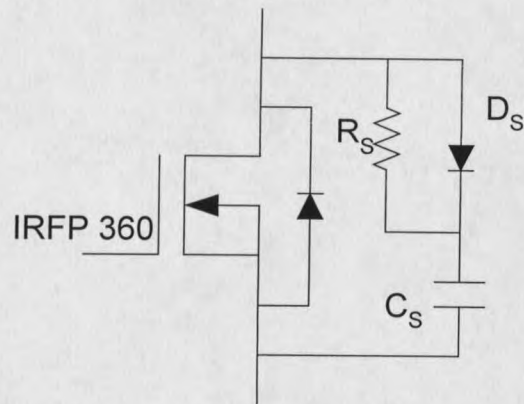


Fig. 4.1: Schematic of the snubber circuit for each mosfet.

Peak voltage stress considerations are explained above. In this application the MOSFET IRFP360 is selected. It has a blocking voltage rating of 400 V and continuous drain current of 23 A.

Eq. 3.1 shows that the switches S_1 and S_2 are complementary switches. Since both the switches can not be ON simultaneously (This would create a short circuit across the output capacitor C_o), a dead time is typically provided, when both S_1 and S_2 are OFF. During this time the boost inductor current flows through the snubber capacitor C_s . The snubber circuit is shown in Fig. 4.1. This is a typical turn OFF Snubber. Capacitor C_s is designed such that the inductor current charges this capacitor to the allowable voltage during the dead time [11]. The resistor R_s limits the turn ON current.

The complete power circuit is presented in Fig. 4.2. The switches S_1 and S_2 are realized with power MOSFET and snubber circuits as described in Fig. 4.1 are added.

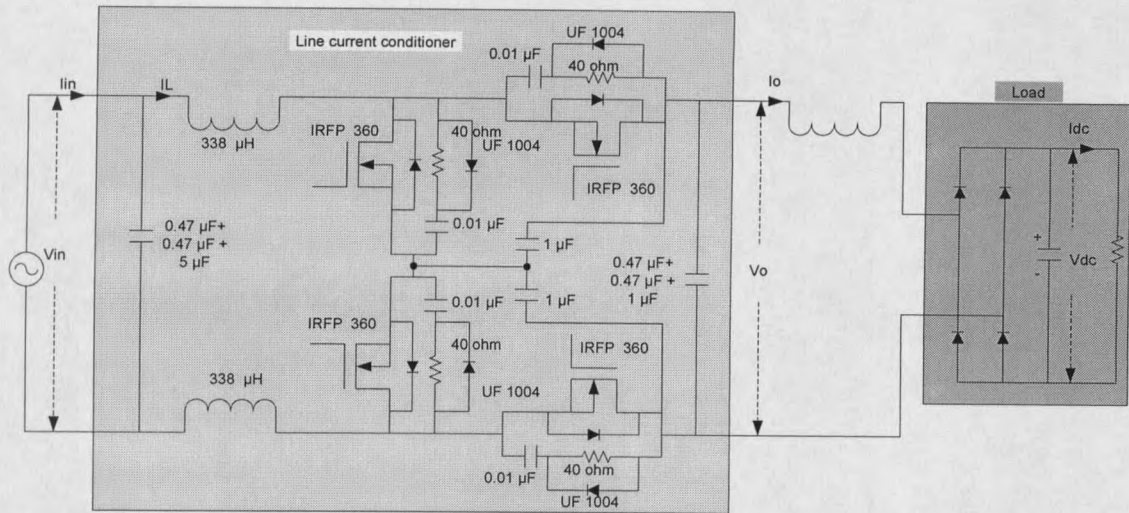


Fig. 4.2: Schematic diagram of complete power circuit.

Conclusion

This chapter concludes the steady state analysis and design. The basic design equations for the boost inductor and equations for determining the rms and average currents through the switches have been provided. The various appendices referred to in this section are useful for developing any similar converter. The next chapter presents the high frequency modeling and dynamic analysis of the converter.

CHAPTER - 5

HIGH FREQUENCY SMALL SIGNAL MODELING AND ANALYSIS

This chapter introduces to the high frequency small signal model of the proposed supply line current conditioner. It is seen that supply voltage is almost constant over a switching cycle so that it could be considered a dc voltage. The model of the averaged current controller is used and suitably modified to represent the circuit used in the implementation of the utility line current conditioner. From the block diagram, the overall loop gain may be computed and used for small signal stability analysis. By using the Bode plot technique, the parameters for the controller may be chosen.

5.1 Model of the Basic Boost Converter

The circuit illustrated in Fig. 3.6 operates from the supply voltage. The switching frequency is 50 kHz whereas the supply frequency is 60 Hz., so that over one or even a few switching cycles the input voltage can be considered as constant and so dc. With these considerations the simplified circuit given in Fig. 3.5 reduces to a simple boost converter as drawn in Fig. 5.1.

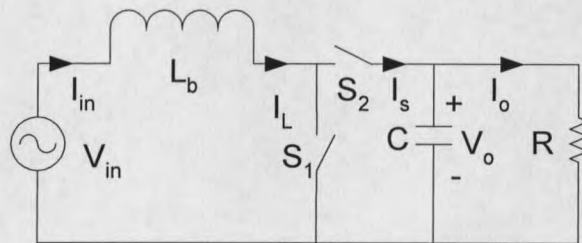


Fig. 5.1: Schematic of the boost converter.

If switching cycle time is T_s , for $0 < t < DT_s$ the switch S1 ON & S2 OFF, for $DT_s < t < T_s$ the switch S1 OFF & S2 ON.

The boost converter is a nonlinear system with respect to the control variable, namely the duty ratio. But in each of the switching intervals DT_s and $(1-D)T_s$ the equivalent circuits are linear. To obtain the equivalent description for the entire switching cycle the defining equations are averaged. From this, it is possible to derive transfer functions for small perturbations around the operating point. The averaging technique and small signal dynamic analysis for switching converters are widely presented in literature. Reference [11] presents a very systematic description of modeling dc to dc power converters. Reference [12] and [13] also provide additional information.

The converter inputs and outputs are shown in Fig. 5.2. V_{in} , I_o and D are inputs and V_o and I_{in} are considered as outputs. Note that I_{in} is considered as an output because the loading and the circuit and its dynamics decide the input current.

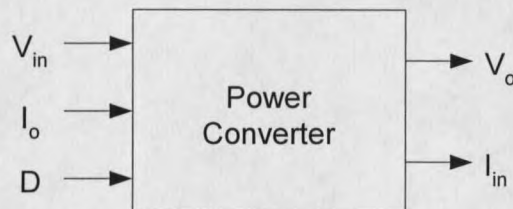


Fig. 5.2: *Input and output variables of the boost converter.*

For small signal analysis we consider small perturbations around the operating point. The small signals are denoted by lower case letters as shown in Fig. 5.3. The operating point is denoted by the corresponding symbols in capital letter.

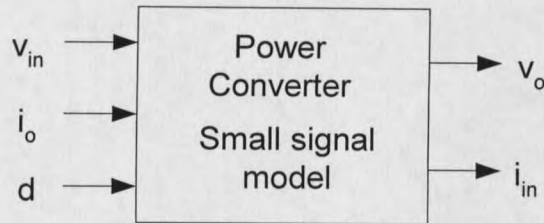


Fig. 5.3: Small signal inputs and outputs of the boost converter.

From Reference [11], the control transfer function of the inductor current may be determined to be,

$$G_b(s) = \frac{i_{in}(s)}{d(s)} = \frac{V_{dc}}{R(1-D)^2} \frac{2 + sCR}{1 + s\frac{L_e}{R} + s^2 L_e C} \quad (5.1)$$

where the parameter L_e is given by

$$L_e = \frac{L_b}{(1-D)^2} \quad (5.2)$$

5.2 Average Current Mode Control

Average current mode control is common in different types of switching power converters and is widely discussed in literature. Reference [8] presents a good summary of the subject. Fig. 5.4 illustrates a common implementation of the scheme. The current controller gives an average signal proportional to the difference between the actual current and the reference current. The current is sensed by measuring the voltage drop across a current sense resistor. Output of the current controller is compared to the saw-tooth wave to generate the duty ratio signal.

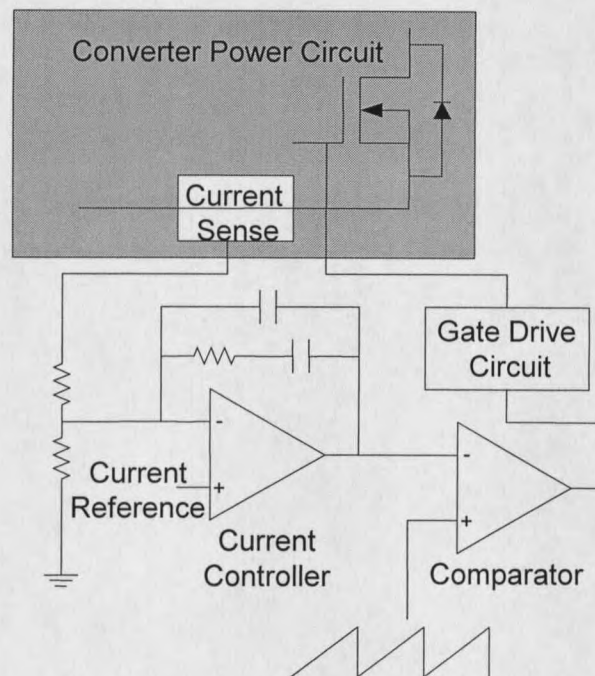


Fig. 5.4: *A general scheme of average current mode control.*

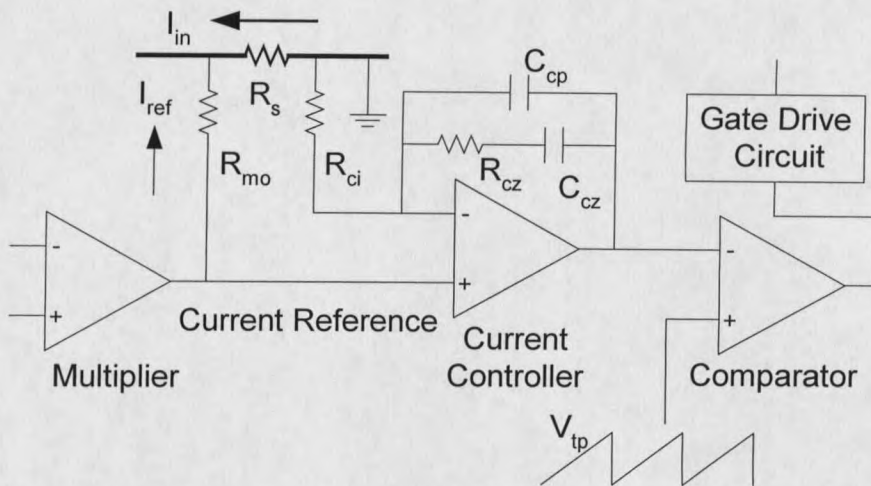


Fig. 5.5: Current controller using UC3854A.

Such a controller may be implemented using the IC UC3854A. The schematic of the current loop of the control circuit is shown in Fig. 5.5. Output of the voltage loop is a multiplier, which gives the reference current to the current loop. The multiplier output is a current source and this current flows through R_{mo} . The load current flows through the sense resistor R_s and generates a negative voltage, which is balanced by the voltage drop in R_{mo} . The current controller amplifier operates with both the inputs near zero voltage. The PI controller produces the signal used to generate the duty ratio.

5.3 Modeling the Current Loop

The current loop consists of the converter, the controller, and the feedback path. The proposed model of the current loop is presented in Fig. 5.6. G_b is the converter transfer function as given in Eq. 5.1.

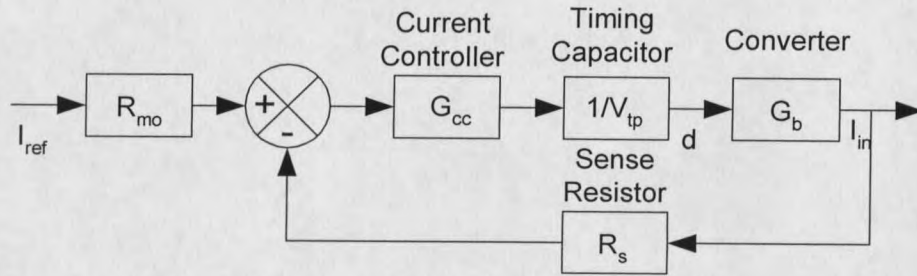


Fig. 5.6: The block diagram of the current loop.

G_{cc} is the transfer function of the PI controller and is given by Eq. 5.3. V_{tp} is the voltage to which the timing capacitor gets charged.

$$G_{cc}(s) = \frac{1 + \frac{s}{\omega_{cz}}}{\frac{s}{\omega_{cpz}} \left(1 + \frac{s}{\omega_{cp}} \right)} \quad (5.3)$$

Where ω_{cz} , ω_{cp} and ω_{cpz} are given by

$$\omega_{cz} = \frac{1}{R_{cz} C_{cz}} \quad (5.4)$$

$$\omega_{cp} = \frac{1}{R_{cz} \frac{C_{cz} C_{cp}}{C_{cz} + C_{cp}}} \quad (5.5)$$

$$\omega_{cpz} = \frac{1}{R_{cz} (C_{cz} + C_{cp})} \quad (5.6)$$

5.4 Loop Stability and Component Selection

With reference to the block diagram of Fig. 5.6 the loop gain function is given by

$$G_{\text{loop}}(s) = G_{\text{cc}}(s) \frac{1}{V_{\text{tp}}} G_{\text{b}}(s) R_{\text{s}} \quad (5.7)$$

It is possible to design the components of the current loop using the loop gain. Bode plot technique has been used for this. Appendix C provides the Mathcad[®] code of the current loop design. Reference [15] provides a detailed step by step discussion for designing ac to dc unity power factor rectifier. For ac to ac application, this approach needs to be modified suitably and the component values could be fine-tuned by using Bode plot technique.

In this application the reference current is modulated at the supply frequency. The current loop response should be fast enough so that the input current tracks the reference current with little error. This requires that the low frequency gain of the current loop should be large and the loop should have a large bandwidth. It should be noted that the operating duty ratio is modulated at double the supply frequency. The loop transfer function is dependent on the operating duty ratio. The stability and performance conditions need to be satisfied ideally for all duty ratios. The following Bode plots are for a duty ratio of 0.8 and 0.2. The steady state gain differs with duty ratio but the stability performances are not affected.

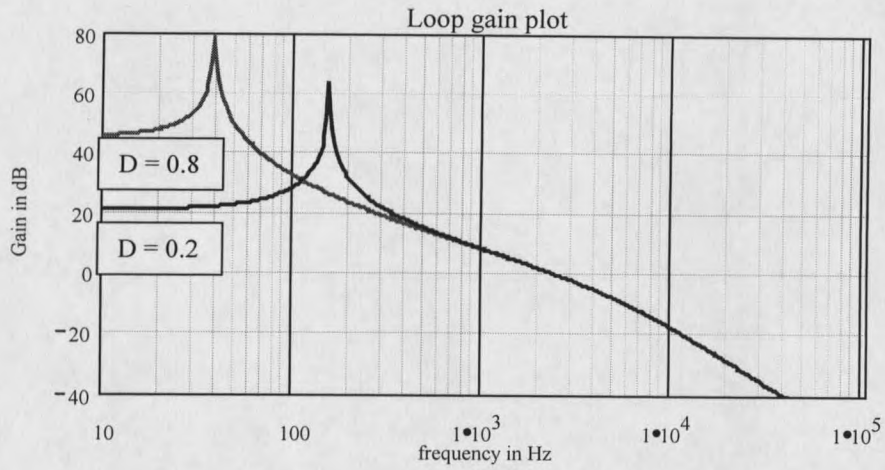


Fig. 5.7: Gain plot of the current loop.

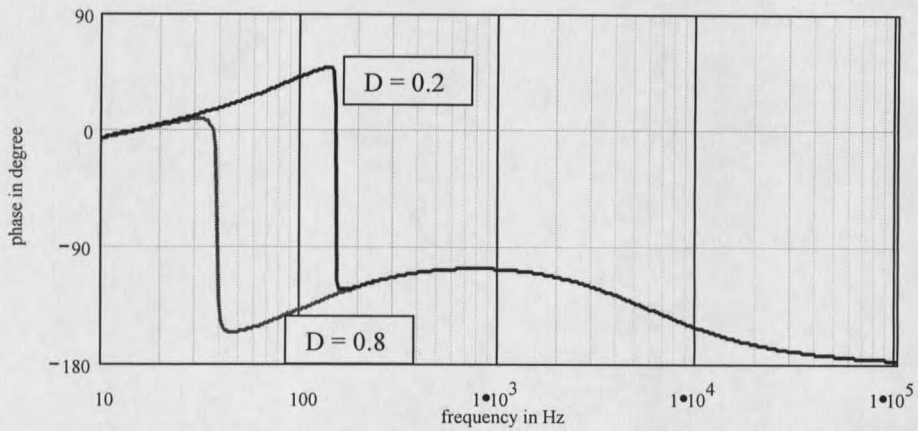


Fig. 5.8: Phase plot of the current loop.

With reference to Fig. 5.5, the above plots are for the following components.

Table – 3 Current controller component values

Symbol	Value
$R_{mo} = R_{ci}$	10 k
R_{cz}	33 k
C_{cz}	0.047 μ F
C_{cp}	880 pF

As seen from the plots that the bandwidth is 2 kHz and the steady low frequency gain is around 46 dB and the phase margin is above 45°. But for duty ratio of 0.8 the phase plot goes close to 180° at a lesser frequency (40 Hz) before the gain cross over frequency. So at that frequency phase stability margin is not very good. However, for a lower duty ratio (0.2) the effect of this phenomenon is less severe.

5.5 Simplified Low Frequency Model of the Current Loop

The block diagram of the current loop could be reduced to find the transfer function between the input current and the reference current. As seen from the Bode plots, the bandwidth of the current loop is around 2 kHz. The dynamics of the whole loop could be neglected and the loop could be considered as a simple gain, for frequencies order of magnitude less than the bandwidth. This is verified by studying the transfer function.

